ORIGINAL RESEARCH

Calpain-Dependent Cleavage of Junctophilin-2 and T-Tubule Remodeling in a Mouse Model of Reversible Heart Failure

Chia-Yen C. Wu, PhD; Biyi Chen, MD, PhD; Ya-Ping Jiang, MD; Zhiheng Jia, PhD; Dwight W. Martin, PhD; Shengnan Liu, BS; Emilia Entcheva, PhD; Long-Sheng Song, MD; Richard Z. Lin, MD

***Background*—**A highly organized transverse tubule (T-tubule) network is necessary for efficient Ca^{2+}-induced Ca^{2+} release and synchronized contraction of ventricular myocytes. Increasing evidence suggests that T-tubule remodeling due to junctophilin-2 (JP-2) downregulation plays a critical role in the progression of heart failure. However, the mechanisms underlying JP-2 dysregulation remain incompletely understood.

***Methods and Results*—**A mouse model of reversible heart failure that is driven by conditional activation of the heterotrimeric G protein $G\alpha_q$ in cardiac myocytes was used in this study. Mice with activated $G\alpha_q$ exhibited disruption of the T-tubule network and defects in Ca^{2+} handling that culminated in heart failure compared with wild-type mice. Activation of $G\alpha_q$/phospholipase Cβ signaling increased the activity of the Ca^{2+}-dependent protease calpain, leading to the proteolytic cleavage of JP-2. A novel calpain cleavage fragment of JP-2 is detected only in hearts with constitutive Gαq signaling to phospholipase Cβ. Termination of the $G\alpha_q$ signal was followed by normalization of the JP-2 protein level, repair of the T-tubule network, improvements in Ca^{2+} handling, and reversal of heart failure. Treatment of mice with a calpain inhibitor prevented $G\alpha_q$-dependent JP-2 cleavage, T-tubule disruption, and the development of heart failure.

***Conclusions*—**Disruption of the T-tubule network in heart failure is a reversible process. $G\alpha_q$-dependent activation of calpain and subsequent proteolysis of JP-2 appear to be the molecular mechanism that leads to T-tubule remodeling, Ca^{2+} handling dysfunction, and progression to heart failure in this mouse model. **(*J Am Heart Assoc*. 2014;3:e000527 doi: 10.1161/JAHA.113.000527)**

Key Words: Calpain • G protein • heart failure • junctophilin-2 • T-tubules

Heart failure is a major chronic illness in the United States, afflicting an estimated 5.7 million Americans and presenting a great economic burden.[1] Drugs used to block the progression of contractile deterioration of the failing heart include the angiotensin-converting enzyme inhibitors. However, current treatments for heart failure are highly unsatisfactory, and the morbidity and mortality from this disease remain high.[2] Therefore, additional insights into the mechanisms that promote the progression of heart failure are urgently needed to provide additional targets for treating this disease.

Cardiac ventricular myocytes contain specialized structures called transverse tubules (T-tubules),[3] which are regularly arrayed invaginations of the plasma membrane. The widely distributed T-tubule network allows rapid and synchronous activation of Ca^{2+} release from the sarcoplasmic reticulum (SR), which is essential for efficient excitation–contraction coupling.[4] T-tubule integrity is thus an important determinant of cardiac function at the cell and organ levels. A number of studies have shown that loss and/or disorganization of T-tubules is part of the phenotypic change in failing hearts of human patients and animal models.[5–14]

Although the exact molecular mechanisms that regulate T-tubule formation and maintenance in cardiac myocytes are still unclear, recent findings indicate that junctophilin-2 (JP-2) is a key regulator of T-tubule structure.[15–17] The JP-2 protein is inserted into the outer membrane surface of the SR and spans the narrow space between T-tubules and the SR.[18] JP-2

From the Departments of Physiology and Biophysics and Institute of Molecular Cardiology (C.-Y.C.W., Y.-P.J., S.L., E.E., R.Z.L.), Medicine and Proteomics Center (D.W.M.), and Biomedical Engineering (Z.J., E.E.), Stony Brook University, Stony Brook, NY; Division of Cardiovascular Medicine, Department of Internal Medicine, University of Iowa Carver College of Medicine, Iowa City, IA (B.C., L.-S.S.); Department of Veterans Affairs Medical Center, Northport, NY (R.Z.L.).

Correspondence to: Long-Sheng Song, MD, Division of Cardiovascular Medicine, Department of Internal Medicine, University of Iowa Carver College of Medicine, Iowa City, IA 52242. E-mail: long-sheng-song@uiowa.edu
Richard Z. Lin, MD, Department of Physiology and Biophysics, Stony Brook University, Stony Brook, NY 11794-8661. E-mail: richard.lin@sunysb.edu

Received September 7, 2013; accepted May 5, 2014.

has been shown to be downregulated or mislocalized in all animal models of heart failure examined and in human heart failure patients.[15,16,19–22] Ablation of JP-2 in cardiac myocytes in vitro and in vivo leads to a disrupted T-tubule network and abnormal Ca^{2+} handling.[15,17,18] More recent studies suggested that microRNA-24 (miR-24) is a direct regulator of JP-2 homeostasis in the heart, and increased expression of miR-24 in failing hearts results in JP-2 downregulation.[23–25] In addition to post-transcriptional regulation, it is yet not well understood how JP-2 is regulated at the post-translational level and how it becomes dysregulated by post-translational modification.[25]

The heterotrimeric G protein $G\alpha_q$ plays a critical role in the development of cardiac hypertrophy and heart failure.[26–28] For example, hormones such as angiotensin II and catecholamines that promote the progression of heart failure activate cell surface receptors that couple to $G\alpha_q$. We previously showed that activation of $G\alpha_q$ in cardiac myocytes of adult mice rapidly leads to heart failure, but the contractile defect is reversed after $G\alpha_q$ signaling is turned off.[29] However, the precise mechanism by which activation of $G\alpha_q$ promotes reversible heart failure remains unclear.

In this study, using a transgenic mouse model of inducible $G\alpha_q$ activity,[30] we demonstrate that activation of $G\alpha_q$ caused JP-2 dysregulation, disruption of T-tubule ultrastructure, and abnormal Ca^{2+} release in cardiomyocytes. Strikingly, abrogation of excessive $G\alpha_q$ activation reversed all of these defects. We also identified a novel calpain cleavage fragment of JP-2 that is detected only in hearts with constitutive $G\alpha_q$ signaling to phospholipase Cβ (PLCβ). Taken together, these data demonstrate that the mechanism by which $G\alpha_q$ induces reversible heart failure is through calpain-dependent cleavage of JP-2 protein and the associated T-tubule network.

Methods

Materials

Ryanodine receptor 2 (RyR2) antibody was obtained from Affinity Bioreagents. 4-[2-[6-(dioctylamino)-2-naphthalenyl] ethenyl]-1-(3-sulfopropyl)-pyridinium (Di-8-ANEPPS), JP-2 antibody for immunostaining, goat anti-rabbit antibody conjugated to Alexa Fluor 488, and goat anti-mouse antibody conjugated to Alexa Fluor 647 were from Invitrogen. MM 4-64 for in situ T-tubule imaging was from AAT Bioquest. JP-2 antibody for Western blotting and immunoprecipitation was from Santa Cruz Biotechnology. Antibody to glyceraldehyde 3-phosphate dehydrogenase (GAPDH) was from Sigma-Aldrich. Calpain inhibitor III, also called MDL 28170, was from Bachem and is reported to be selective for calpains I and II.[31] ECL secondary antibodies were from GE Healthcare. Fodrin antibody was purchased from Cell Signaling Technology.

Animals

Transgenic C57BL/6 mice expressing $G\alpha_q$Q209L-hbER (referred to as QL) and $G\alpha_q$Q209L-hbER with the R256A and T257A substitutions (referred to as AA) under the control of an α myosin heavy chain promoter were described previously.[30] The transgenic proteins are expressed in cardiac myocytes from birth. By fusing a mutant hormone-binding domain of the estrogen receptor (hbER)[2] at the C-terminus of the transgenic proteins, they remain inactive until the mice are injected with tamoxifen. Mice 2 to 3 months of age were injected daily with 1 mg of tamoxifen suspended in peanut oil with or without 500 μg of calpain inhibitor III dissolved in DMSO. All animal-related experimental protocols for this study were approved by the Institutional Animal Care and Use Committee of Stony Brook University and the University of Iowa.

Echocardiography

Mice were anesthetized with 1% to 2% isoflurane, and transthoracic echocardiography was performed as previously described.[32]

T-tubule Visualization

In situ T-tubule imaging and Fourier analysis of T-tubule integrity were performed as previously described.[15] Peak power was measured as the absolute value using Gaussian fitting with Clampfit (Molecular Devices) as previously reported.[15] Cardiac ventricular myocytes were isolated as described previously.[33] T-tubule imaging, immunofluorescence confocal microscopy, and one-dimensional Fourier analysis on isolated cardiac ventricular myocytes were performed as previously described.[16]

Whole Heart Ca^{2+} Transient and Myocyte SR Ca^{2+} Content Measurements

In situ Ca^{2+} imaging of physiologically coupled myocytes was performed in Langendorff-perfused intact hearts as previously described.[34,35] SR Ca^{2+} content measurement in isolated myocytes in response to caffeine stimulation was performed as previously described.[36]

Western Blotting

Mouse heart lysates were prepared in general lysis buffer (50 mmol/L HEPES, 2% Triton X-100, 50 mmol/L NaCl, 5 mmol/L EDTA, 50 mmol/L NaF, 10 mmol/L sodium pyrophosphate, 1 mmol/L sodium orthovandate, 0.5 mmol/L phenylmethylsulfonyl fluoride, and 10 μg/mL each of aprotinin and leupeptin, pH 7.5). After immunoblotting, signals were visualized using an ECL kit (PerkinElmer Life Sciences).

In-gel Digestion and Protein Identification

A frozen heart sample from a 2-month-old QL mouse injected with tamoxifen for 2 weeks was homogenized in general lysis buffer. Two samples (1 mg lysate protein and immunoprecipitated product from 12 mg lysate protein) were diluted 1:1 in Bio-Rad 2× Laemmeli sample buffer containing 5% 2-mercaptoethanol, heated 5 minutes at 95°C, and loaded into separate wells of a Bio-Rad Criterion Tris-HCl polyacrylamide gel (10% resolving gel and 4% stacking gel). After electrophoresis, the section of the gel containing the lysate lane was cut off and used for JP-2 immunoblotting. The remainder of the slab gel was stained with SYPRO Ruby Stain according to the Bio-Rad instruction manual and imaged with use of a Bio-Rad VersaDoc 3000 Imaging System.

The images of the JP-2 immunoblot and the stained gel were aligned, and the regions corresponding to the immunostained bands were excised from the gel using a Bio-Rad ProteomeWorks Plus Spot Cutter with a 1.5-mm cutting tip. The gel pieces were placed into wells of a 96-well plate, along with comparably sized pieces of blank regions of the gel that served as background references during sample processing. The excised gel pieces were destained, reduced, alkylated, and digested with trypsin (Promega Gold, Mass Spectrometry Grade). The resulting concentrated peptide extract was diluted into a solution of 2% acetonitrile (ACN), 0.1% formic acid (FA) (buffer A) for analysis. The peptide mixture was analyzed by automated microcaplillary liquid chromatography–tandem mass spectrometry. Fused-silica capillaries (100-μm internal diameter) were pulled using a P-2000 CO_2 laser puller (Sutter Instruments) to a 5-μm internal diameter tip and packed with 10 cm of 5-μm Magic C18 material (Agilent) using a pressure bomb. The column was then placed in-line with a Dionex Ultimate 3000 equipped with an autosampler. The column was equilibrated in buffer A, and the peptide mixture was loaded onto the column using the autosampler. The HPLC pump flowed at 100 μL/min, and the flow rate to the electrospray tip was reduced to ≈200 to 300 nL/min by a split. The HPLC separation was provided by a gradient between buffer A and buffer B (98% ACN, 0.1% FA). The HPLC gradient was held constant at 100% buffer A for 20 minutes after peptide loading followed by a 30-minute gradient to 40% buffer B. Then the gradient was switched from 40% to 80% buffer B over 3 minutes and held constant for 3 minutes. Finally, the gradient was changed from 80% buffer B to 100% buffer A over 1 minute and then held constant at 100% buffer A for 40 additional minutes. The application of a 1.8-kV distal voltage electrosprayed the eluted peptides directly into a Thermo Fisher Scientific LTQ XL ion trap mass spectrometer equipped with a nanoLC electrospray ionization source (ThermoFinningan). Full mass spectra (MS) were recorded on the peptides over a 400- to 2000-*m/z* range, followed by five tandem mass (MS/MS) events sequentially generated in a data-dependent manner on the first, second, third, fourth, and fifth most intense ions selected from the full MS spectrum (at 35% collision energy). Mass spectrometer scan functions and HPLC solvent gradients were controlled by the Xcalibur data system (ThermoFinnigan).

MS/MS spectra were extracted from the RAW file with the use of Readw.exe (http://sourceforge.net/projects/sashimi). The resulting mzXML file contains all the data for all MS/MS spectra. The MS/MS data were searched with the use of Inspect[37] against an IPI mouse database with optional modifications: +16 on methionine, +57 on cysteine, and +80 on threonine, serine, and tyrosine. Only peptides with a $P \leq 0.01$ value were analyzed further. Common contaminants (eg, keratins) were removed from the database. Proteins identified by at least 2 distinct peptides were accepted for a valid identification.

Calpain Activity Assay

Calpain activity was assayed using the BioVision Calpain Activity Assay kit. Heart tissue was homogenized in the extraction buffer supplied with the kit, incubated on ice for 20 minutes, and then centrifuged at 10 000*g* at 4°C. Then, 50 μg of protein in the supernatant was diluted in the extraction buffer and mixed with reaction buffer and calpain substrate. Samples were incubated at 37°C, and readings were taken every 400 seconds for 1 hour in a microplate fluorescence reader (excitation of 360 nm and emission of 520 nm).

Statistics

Data were expressed as mean±SEM. The Student *t* test was used for analysis of T-tubule peak power (Figure 5B), JP2 power spectra (Figure 6B), and JP-2/RyR2 colocalization (Figure 6C). All Western blot data (Figures 7A and 10A, 10B) and calpain activity assay (Figure 9A) were analyzed by using Mann–Whitney *U* test or Kruskal–Wallis test; one-way ANOVA with Bonferroni post-test was used to analyze T-tubule peak power (Figure 11B) and JP-2/RyR2 colocalization (Figure 11C); and linear mixed-effects models test was used for analysis of Ca^{2+} transient parameters (Figures 2B, 2D and 3B, 3C) and TT_{power} (Figure 4B) from intact hearts. The Pearson correlation statistics was used in Figure 6C to assess correlation between groups. Statistical analysis was carried out using SPSS V 15.0, and $P<0.05$ was considered statistically significant.

Results

Reversibility of $G\alpha_q$-Induced Heart Failure

In a previous study, we showed that transgenic mice expressing the $G\alpha_q$Q209L-hbER protein (abbreviated as QL mice hereafter)

rapidly developed decompensated heart failure when injected with tamoxifen to activate $G\alpha_q$ signaling.[30] In this study, we sought to better understand the molecular mechanisms of heart failure development induced by $G\alpha_q$ activation in this animal model. We first demonstrated the reversibility of heart failure in the QL mice by performing serial echocardiographic examinations of wild-type (WT) and QL mice before tamoxifen injection ("Baseline"), after 2 weeks of daily injections ("Tamoxifen"), and 3 weeks after the last drug injection ("Recovery"). Shown in Figure 1A are M-mode echocardiograms obtained from 1 representative WT and 1 representative QL animal at the 3 treatment stages. Before tamoxifen injection, the QL mice had normal cardiac contractility as measured by fractional shortening (Figure 1B). Two weeks of tamoxifen injections induced dramatic decreases in fractional shortening in all of the QL mice but did not have significant negative effects on the WT mice (Figure 1B). Three weeks after the cessation of tamoxifen injections, cardiac contractility in all of the QL mice recovered to baseline levels (Figure 1B). The QL mice also developed a substantial increase in left ventricular volume that improved during the recovery period, as shown in Figure 1B. Tamoxifen did not increase the left ventricular

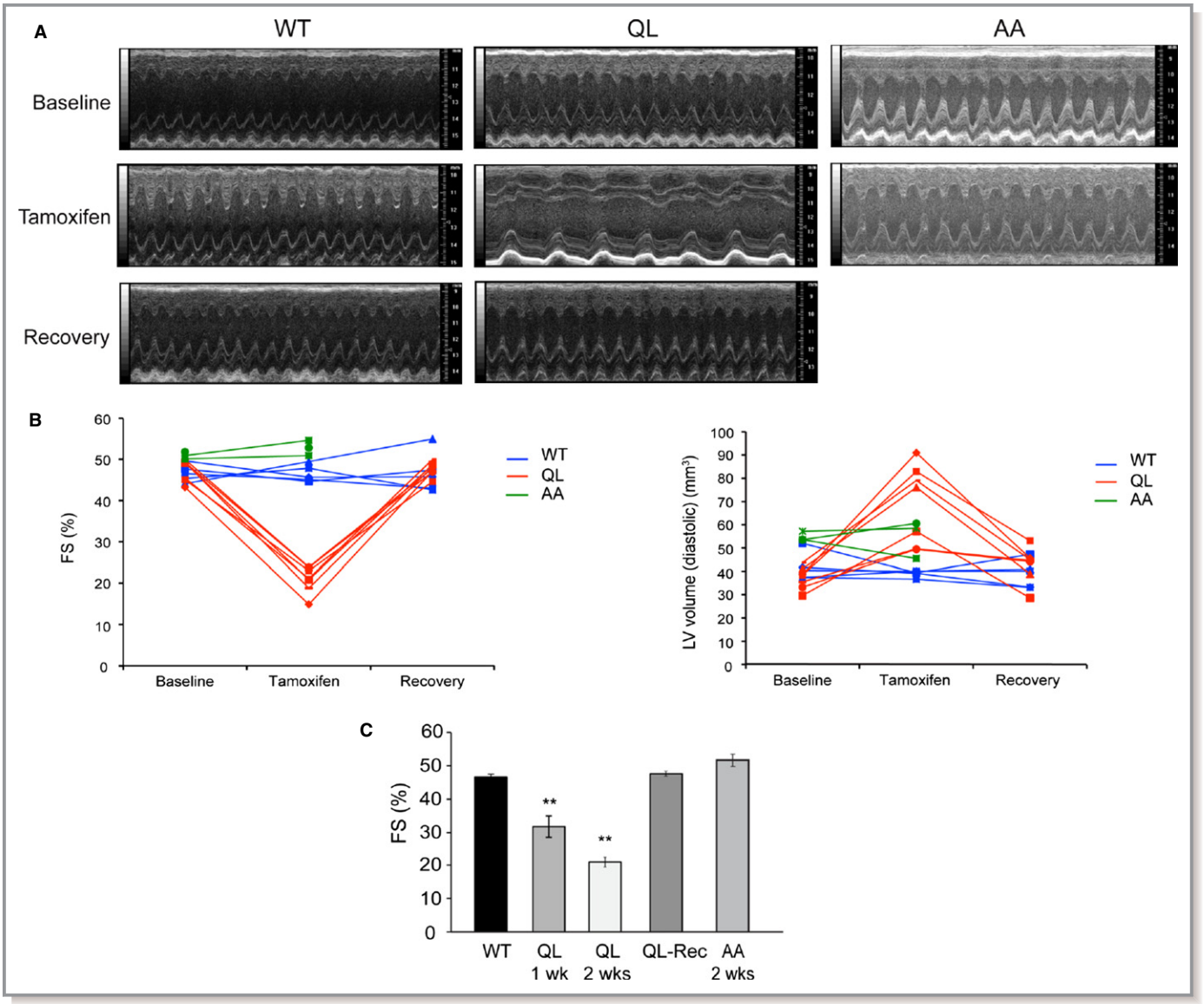

Figure 1. Conditional activation of $G\alpha_q$ causes reversible heart failure. A, M-mode transthoracic views of 1 representative WT, 1 representative QL mouse, and 1 representative AA mouse before treatment with tamoxifen (Baseline), after 2 weeks of tamoxifen injections (Tamoxifen), and 3 weeks after the final tamoxifen injection (Recovery). B, Percent fractional shortening (FS) and left ventricular (LV) volume (mm^3) for 5 WT, 7 QL, and 3 AA mice at the 3 treatment stages. C, Summary of % FS from mice of the following groups: WT (n=5), QL after 1 week of tamoxifen (n=3), QL (n=7) and AA (n=3) after 2 weeks of tamoxifen, and QL after 3-week recovery (QL-Rec, n=7). ** $P<0.01$ compared with WT-tamoxifen. Data shown are mean±SEM. WT indicates wild-type.

Table 1. Echocardiographic Measurements of Mice Injected for 2 Weeks

	Baseline			Tamoxifen			Tamoxifen+Calpain Inhibitor	Recovery	
	WT	QL	AA	WT	QL	AA	QL	WT	QL
LVEDD, mm	3.28±0.05	3.07±0.03	3.61±0.03	3.38±0.06	3.97±0.06*	3.60±0.03	3.43±0.04†	3.30±0.05	3.25±0.04‡
LVESD, mm	1.82±0.06	1.62±0.03	1.77±0.03	1.75±0.05	3.16±0.07*	1.70±0.03	1.89±0.04†	1.76±0.05	1.73±0.03‡
PWT, mm	0.97±0.03	0.91±0.02	0.80±0.02	1.00±0.03	0.82±0.03*	0.86±0.03	0.73±0.03	0.91±0.03	1.00±0.03‡
FS, %	46.6±1.5	47.3±0.8	50.9±0.64	46.5±1.3	20.9±1.3*	52.8±0.43	45.4±0.8†	46.7±1.3	47.6±1.1‡
HR, bpm	523.9±18.2	500.6±27.1	454.6±2.36	487.7±6.1	262.2±23.6*	448.2±3.53	370.6±17.0†	557.5±13.7	551.0±11.1‡

Values are means±SEM. Serial echocardiographic examinations were done on 5 WT and 7 QL mice at the 3 treatment stages (Baseline, Tamoxifen, and Recovery). A separate group of QL mice (n=7) was examined after 2 weeks of daily injections with tamoxifen plus calpain inhibitor. Three AA mice were also studied before and after tamoxifen injection. bpm indicates beats per minute; FS, fractional shortening; HR, heart rates; LVEDD, left ventricular end-diastolic diameter; LVESD, left ventricular end-systolic diameter; PWT, posterior wall thickness; WT, wild-type.
*P<0.01 compared with WT-tamoxifen; †P<0.01 for the comparison of calpain inhibitor treated group to QL-tamoxifen group. ‡P<0.01 for the comparison of QL-recovery group to QL-tamoxifen group.

volume of WT mice (Figure 1B). Table 1 summarizes the serial echocardiograhic data from both groups of mice. It should be noted that when QL mice died during the 2 weeks of tamoxifen injections, as we previously reported,[30] the data from those animals were not included in the study.

We performed additional experiments with WT and QL mice that were injected with tamoxifen for only 1 week. At this time point, the contractile abnormality of the QL mice as measured by echocardiography was not as severe as that observed after 2 weeks of injections (Table 2). Figure 1C summarizes the contractile changes of QL mice under the various conditions. The cardiac contractility of QL mice injected for 1 week with tamoxifen was decreased by 37% compared with the WT group, whereas the contractility of QL mice injected for 2 weeks was reduced by 55%. These data indicate that taxmoxifen-induced activation of $G\alpha_q$ signaling causes a progressive reduction in cardiac contractile function.

Abnormal Ca^{2+} Handling in $G\alpha_q$-induced Heart Failure

Heart failure is often associated with defective Ca^{2+} handling in myocytes.[38] To investigate Ca^{2+} handling in QL mice with heart failure, in situ imaging of Ca^{2+} transients was performed in intact WT and QL hearts after 1 or 2 weeks of tamoxifen injections and in QL hearts after 3 weeks of recovery. Figure 2A shows representative Ca^{2+} transient images obtained from spontaneously beating hearts, and Figure 2C shows images obtained from hearts paced at 5 Hz. Note that the spontaneous rate of the QL-tamoxifen heart was slower than that of the WT-tamoxifen heart (Figure 2A; also see Tables 1 and 2). Ca^{2+} transient amplitude in hearts from QL mice treated with tamoxifen for 1 week was significantly reduced compared with the WT-tamoxifen group (Figure 2B and 2D). The reduction in Ca^{2+} transient amplitude was more severe in QL mice injected for 2 weeks (Figure 2B and 2D). This defect

Table 2. Echocardiographic Measurements of Mice Injected With Tamoxifen for 1 Week

	Basal		Tamoxifen 1 Week	
	WT	QL	WT	QL
LVEDD, mm	3.31±0.05	3.55±0.08	3.62±0.05	3.74±0.07
LVESD, mm	1.68±0.03	1.74±0.07	1.69±0.03	2.56±0.07*
PWT, mm	0.75±0.02	0.74±0.03	0.71±0.02	0.83±0.04
FS, %	49.1±0.9	50.7±1.54	50.6±0.93	31.8±1.89*
HR, bpm	486.2±25.2	464.3±9.6	447.0±8.9	333.5±40.0*

Values are mean±SEM. Serial echocardiographic examinations were done on 3 WT and 3 QL mice at the 2 treatment stages (Basal and Tamoxifen 1 week). WT indicates wild-type; LVEDD, left ventricular end-diastolic diameter; LVESD, left ventricular end-systolic diameter; PWT, posterior wall thickness; FS, fractional shortening; HR, heart rates; bpm, beats per minute.
*P<0.01; compared with WT-tamoxifen.

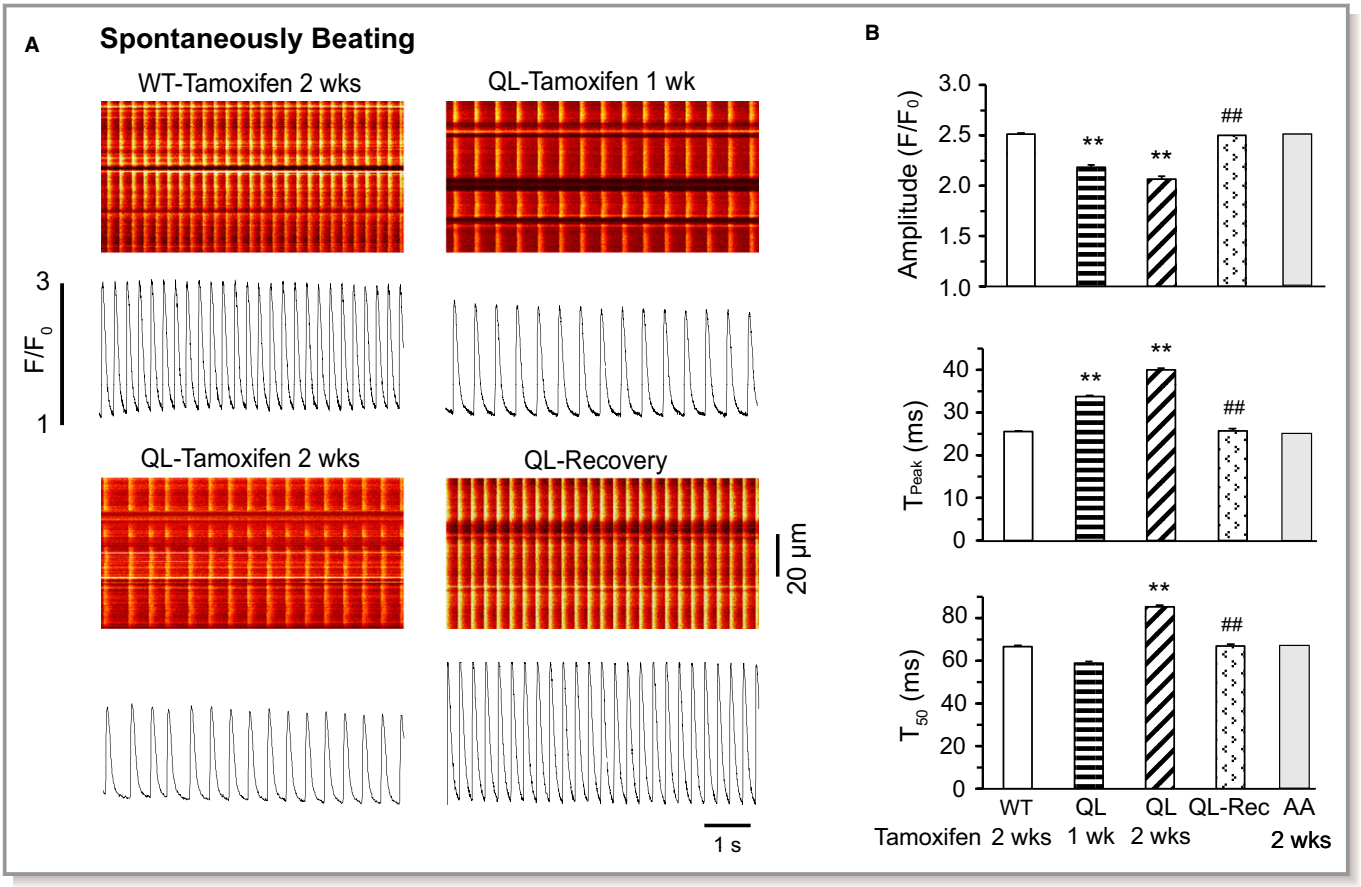

Figure 2. Decreased amplitude and slowed kinetics of Ca^{2+} transients in QL hearts. Ca^{2+} transients were imaged in situ in hearts prepared from tamoxifen-treated WT, QL (1 or 2 weeks), and AA mice and from QL mice 3 weeks after the last tamoxifen injection (QL-recovery). A, Representative images of Ca^{2+} transients in spontaneously beating hearts. B, Summary of Ca^{2+} transient parameters derived from data collected as in (A): amplitude (F/F_0), time to peak (T_{peak}), and time from peak to 50% decay (T_{50}). $^{**}P<0.01$ compared with WT-tamoxifen; $^{\#}P<0.05$ compared with QL-tamoxifen 2 weeks by linear mixed-effects models test. C, Representative images of external stimulation (5 Hz)–triggered Ca^{2+} transients. D, Summary of Ca^{2+} transient parameters derived from data collected as in (C). $^{**}P<0.01$ compared with WT-tamoxifen; $^{\#}P<0.05$ compared with QL-tamoxifen 2 weeks by linear mixed-effects models test, mean±SEM, n=223 cells for WT, n=201 cells for QL 1 week, n=280 cells for QL 2 weeks,: n=288 cells for QL-Rec from 3 hearts for each group, respectively. WT indicates wild-type.

was completely reversed in the QL-recovery hearts (Figure 2B and 2D). In addition, the time needed to reach peak Ca^{2+} amplitude (T_{peak}) was markedly increased in spontaneously beating or paced QL-tamoxifen hearts, and this alteration was also completely reversed in the QL-recovery hearts (Figure 2B and 2D). Again, this defect was more severe in QL mice injected with tamoxifen for 2 weeks than in mice injected for 1 week (Figure 2B). The time from peak to 50% decay of the Ca^{2+} signal (T_{50}) was also significantly longer in spontaneously beating QL hearts from mice injected for 2 weeks, but not for 1 week, compared with WT (Figure 2B). However, this difference was eliminated when the WT and QL hearts were paced at the same rate (5 Hz), suggesting that the decelerated decay of Ca^{2+} transients is frequency dependent (Figure 2D).

Similar to what we found in the whole heart, isolated QL-tamoxifen myocytes paced at either 1 Hz or 3 Hz also exhibited a marked decrease in Ca^{2+} transient amplitude, an increase in T_{peak}, and no significant difference in T_{50} compared with WT-tamoxifen cells (Figure 3A and 3B). We next investigated whether a decrease in SR Ca^{2+} content might account for the defect in Ca^{2+} handling caused by activation of $G\alpha_q$. Isolated myocytes were paced at 1 Hz and then treated with caffeine to release the SR store Ca^{2+}. The amplitude of caffeine-induced Ca^{2+} release from the SR was minimally affected in the QL-tamoxifen versus the WT-tamoxifen myocytes (Figure 3C and 3D).

$G\alpha_q$ activates PLCβ to generate diacylglycerol and inositol trisphosphate (IP_3), 2 second messengers that cause an increase in protein kinase C activity and Ca^{2+} release, respectively.[39] We previously generated transgenic mice with cardiac myocyte-specific expression of a $G\alpha_q$ Q209L-hbER protein with alanine substitutions at amino acids Arg256 and Thr257.[30] This mutant (referred to as AA) cannot activate PLCβ.[30] Calcium transient parameters in hearts of tamoxifen-

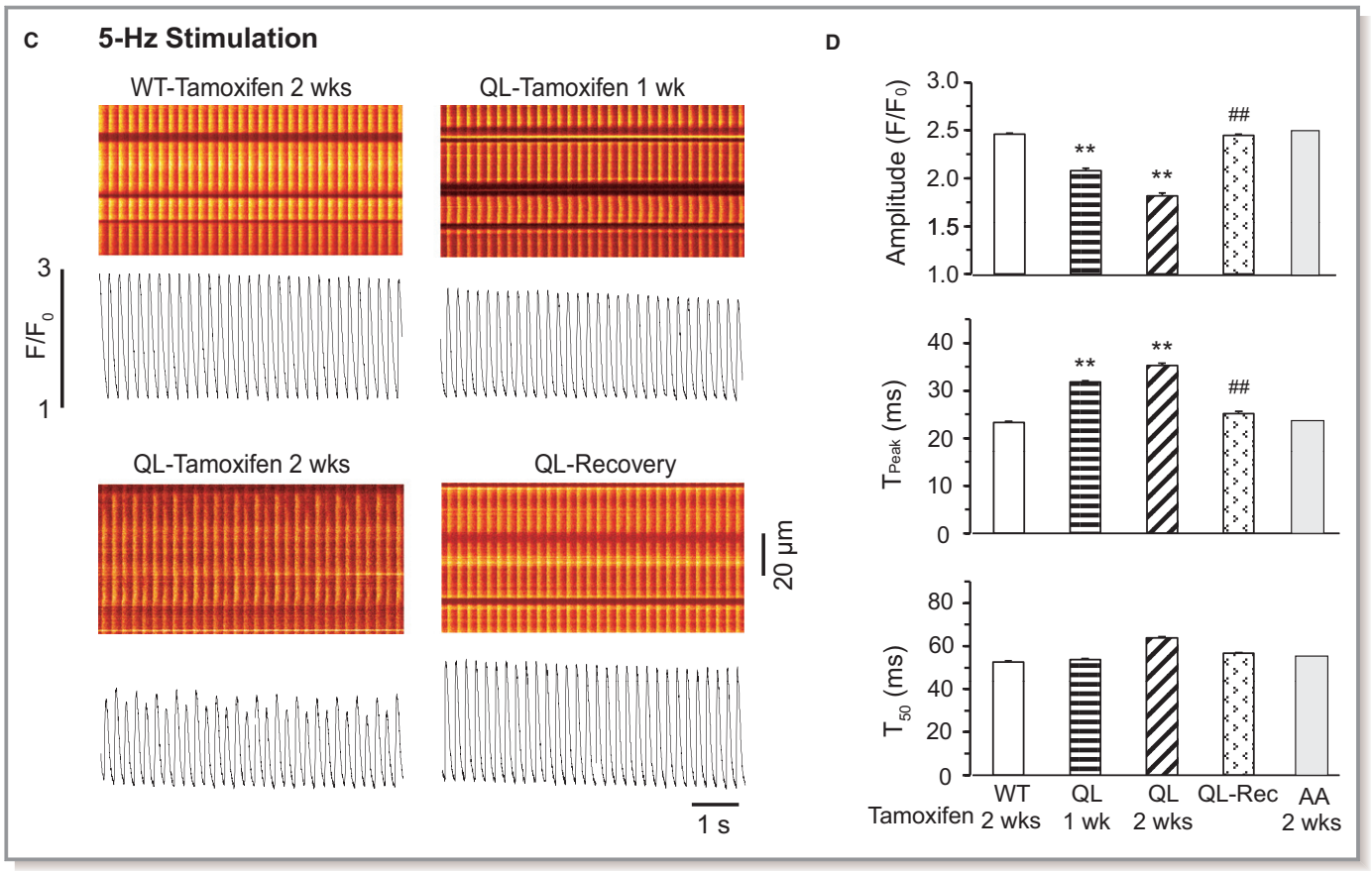

Figure 2. Continued.

injected AA mice were similar to those of the WT-tamoxifen hearts (Figure 2). Echocardiographic examination of AA mice before and after 2 weeks of tamoxifen injections showed that fractional shortening and other left ventricular measurements did not change significantly (Figure 1 and Table 1). These results indicate that activation of PLCβ is required for the development of heart failure in QL mice.

Reversible T-tubule Disruption

T-tubule structure is an important determinant of cardiac excitation–contraction coupling function.[4,40] To determine whether T-tubule remodeling occurs in QL mice with heart failure, we mounted hearts on a Langendorff apparatus, perfused them with a lipophilic dye (MM 4-64; AAT Bioquest) that stains the plasma membrane, and used in situ confocal imaging to visualize T-tubules in left ventricular epicardial myocytes of the intact hearts.[15,16] Figure 4A shows representative images of WT and QL hearts. When compared with WT-tamoxifen hearts, myocytes in hearts of the QL mice injected with tamoxifen for 1 week exhibited a slightly disorganized pattern of T-tubules, with a statistically significant decrease in power at the dominant frequency as analyzed by two-dimensional Fourier transform (Figure 4A and 4B). However, after 2 weeks of tamoxifen treatment, the T-tubule network of QL myocytes exhibited markedly disorganized pattern, giving rise to an overall chaotic appearance of the T-tubule network and, hence, low spatial periodicity. Power spectrum analysis using two-dimensional Fourier transform yielded much lower power at the dominant frequency in the 2-week QL-tamoxifen group (Figure 4A and 4B). This defect was almost completely reversed in the hearts of QL mice after 3 weeks of recovery (Figure 4A and 4B). Additional histogram analysis of the images showed that most of the images in the tamoxifen-treated WT group had highly organized T-tubules whose TT_{power} fell in the 2.0 to 2.6 range, whereas the majority of 2-week QL-tamoxifen cells exhibited power of <1.7 (Figure 4C) and most of the 1-week QL-tamoxifen myocytes exhibited TT_{power} that fell between those for 2-week QL-tamoxifen and WT-tamoxifen cells (Figure 4C). Although T-tubules in most of the QL-recovery myocytes were highly organized with TT_{power} of >2.0, some of them still had disrupted T-tubules whose TT_{power} fell into the 1.4 to 1.7 bin range (Figure 4C). Data from additional T-tubule imaging experiments using isolated myocytes (Figure 5) are consistent with those obtained using in situ imaging from intact hearts. In

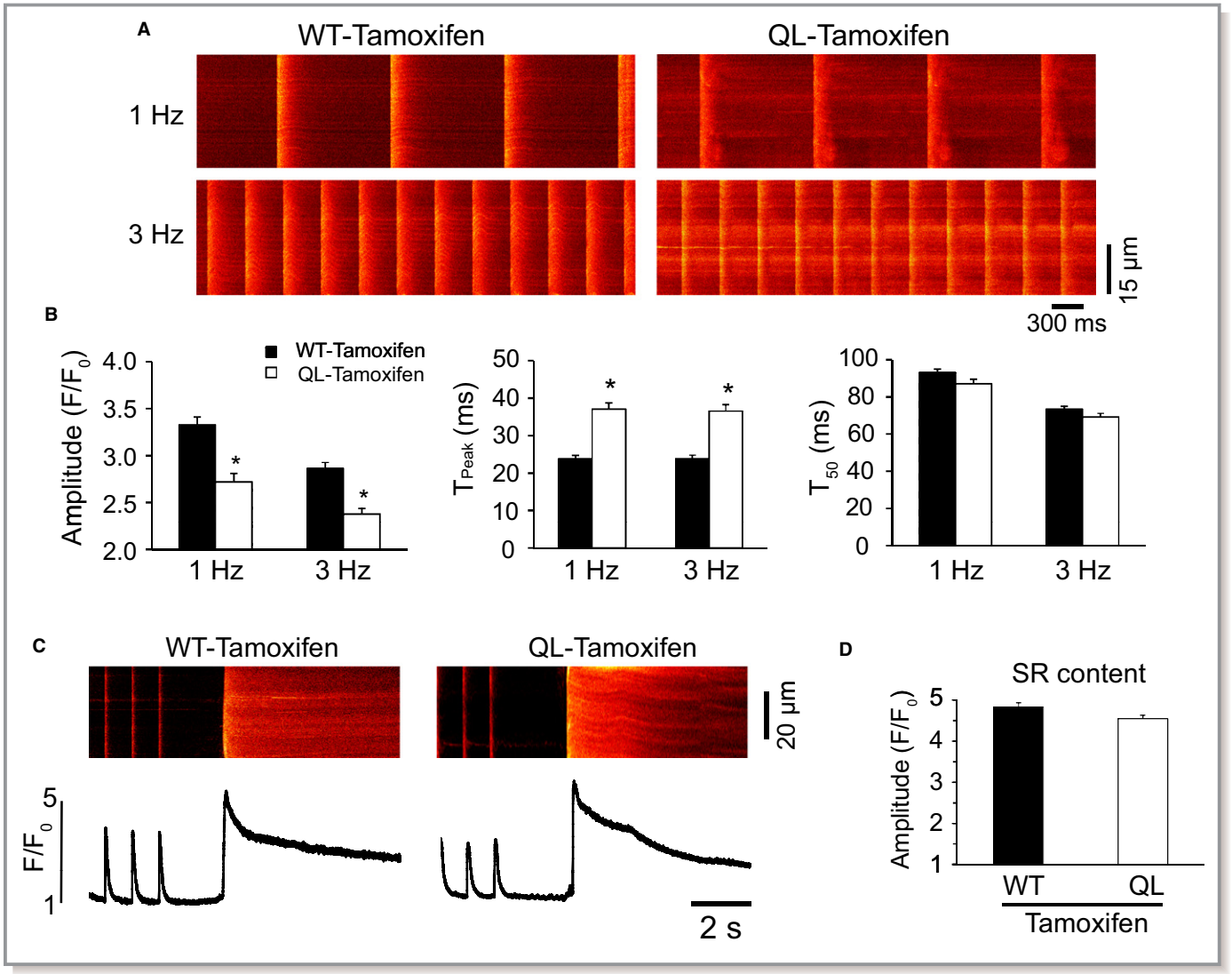

Figure 3. Field stimulation (1 and 3 Hz)–triggered Ca^{2+} transients from myocytes of tamoxifen-treated WT and QL mice. A, Representative images of Ca^{2+} transients. B, Summary of Ca^{2+} transients: Amplitude (F/F_0), time to peak (T_{Peak}), and decay rate (T_{50}). *P<0.05, vs WT by linear mixed-effects models test, mean±SEM, n=52 cells for WT, n=65 cells for QL from 3 hearts for each group, respectively. C&D, Field stimulation (1 Hz)–triggered Ca^{2+} transients and caffeine-induced Ca^{2+} release (SR content) from myocytes of tamoxifen-treated WT and QL mice and summary of SR Ca^{2+} content. *P<0.05 vs WT by linear mixed-effects models test, mean±SEM, n=72 cells for WT, n=69 cells for QL from 3 hearts for each group, respectively. WT indicates wild-type.

contrast to QL-tamoxifen myocytes, myocytes from AA-tamoxifen mice exhibited an organized T-tubule pattern (Figure 5C). Taken together, our data indicate that $G\alpha_q$ activation of PLCβ is the mechanism that causes T-tubule disruption in QL hearts.

JP-2 Abnormalities Due to Activation of $G\alpha_q$

JP-2 plays a critical role in regulating T-tubule organization in cardiac myocytes.[15–17] We recently reported that genetic ablation of 2 phosphoinositide 3-kinases in cardiac myocytes led to decompensated heart failure in mice and altered localization of JP-2 with no change in protein expression.[16] Therefore, we used immunofluorescence microscopy to determine whether JP-2 is also mislocalized in myocytes of QL mice with heart failure. As expected, staining of JP-2 in cardiomyocytes from tamoxifen-injected WT mice showed an orderly striated pattern that strongly overlapped with RyR staining (Figure 6A). In contrast, JP-2 in QL-tamoxifen myocytes did not show a striated distribution with a constant periodic spacing (Figure 6A). The lack of periodicity was reflected by the low normalized power calculated from the one-dimensional Fourier transform of the staining signal (Figure 6B). JP-2 colocalization with RyR was also reduced in the QL-tamoxifen myocytes (Figure 6C). The striated arrangement of JP-2 and JP-2 colocalization with RyR were

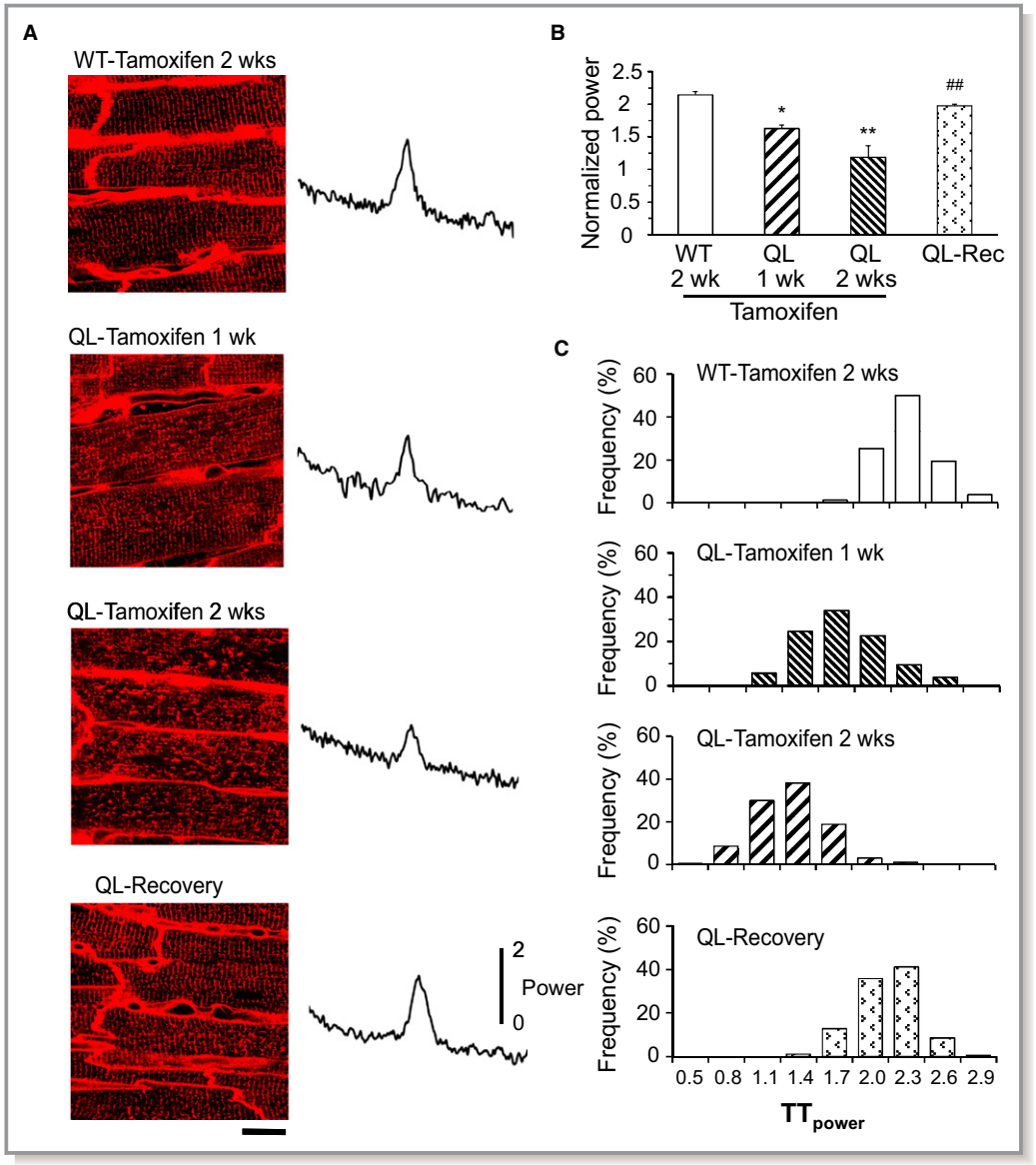

Figure 4. Disruption of the T-tubule network in QL hearts. A, In situ imaging of T-tubules in the left ventricle of intact WT-tamoxifen, QL-tamoxifen (1 or 2 weeks), and QL-recovery hearts perfused with MM 4-64. Representative power spectrum of spatial frequency for each group was shown next to the T-tubule images. B, T-tubule organization was analyzed by two-dimensional Fourier transform of the MM 4-64 image to calculate the strength of T-tubule regularity (TT_{power}). $^{**}P<0.01$ vs WT, $^{\#\#}P<0.01$ vs QL 2 weeks by linear mixed-effects models test, mean±SEM, n=75 images, 5 hearts for WT, n=45 images, 3 hearts for QL 1 week, n=90 images, 6 hearts for QL 2 weeks, respectively. C, Histogram distribution of TT_{power} from individual frame of T-tubule images from left ventricles. WT indicates wild-type.

restored in the QL myocytes after 3 weeks of recovery (Figure 6).

Western blotting showed that there was a marked decrease in the level of full-length JP-2 in heart lysates of QL-tamoxifen mice compared with WT-tamoxifen animals (Figure 7A and 7B). Interestingly, a cleaved form of JP-2 was detected in the QL-tamoxifen hearts (Figure 7A). This JP-2 cleavage product was also seen in hearts of QL mice collected after only 7 days of tamoxifen injections (Figure 7A). At this time point, the level of full-length protein was not reduced in the QL hearts, suggesting a compensatory response to increased cleavage of JP-2 (Figure 7A). In contrast, tamoxifen injection of AA mice for 2 weeks did not cause a decrease in the expression of JP-2 or induce the cleaved form of this protein in heart lysates (Figure 7B). The expression level of full-length JP-2 in QL hearts returned to WT levels after 3 weeks of recovery from the tamoxifen injections, and the cleaved form of JP-2 was no longer detected (Figure 7A).

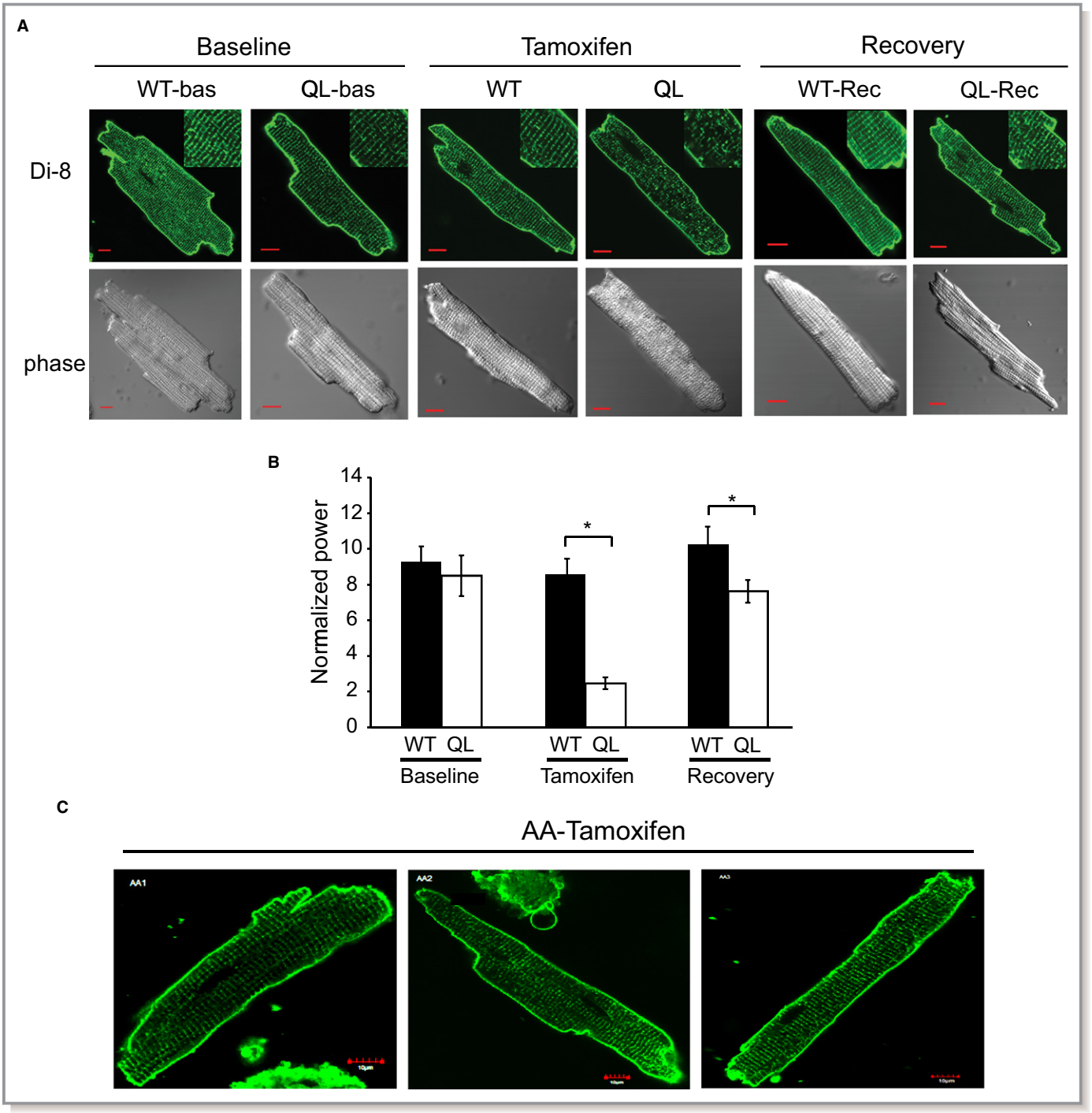

Figure 5. Disruption of the T-tubule network in single QL cardiomyocytes. A, Representative confocal microscopy images of cardiac myocytes isolated from untreated WT and QL mice (Baseline), mice injected for 2 weeks with tamoxifen (Tamoxifen), and mice allowed to recover for 3 weeks after the last tamoxifen injection (Recovery). Myocytes were stained with di-8-ANEPPS. Phase contrast images of the same cells are displayed in the bottom panels. Scale bars are 10 μm. The insets show ×2 magnified views. B, Normalized peak power (at the dominant frequency) computed from one-dimensional Fourier analysis of the di-8-ANEPPS signal as a measure of T-tubule spatial organization. Data are mean±SEM (n=16 to 27 cells from ≥3 hearts per group; **P*<0.01, Student's *t* test). C, Representative confocal microscopy images of cardiac myocytes isolated from 3 AA mice treated with tamoxifen for 2 weeks. Myocytes were stained with di-8-ANEPPS. WT indicates wild-type.

Taken together, these results indicate that JP-2 protein localization and expression are both altered during the development of $G\alpha_q$-induced heart failure. Furthermore, the JP-2 abnormality is a reversible process. Our data also suggest that PLCβ activation is required for $G\alpha_q$-induced JP2 cleavage.

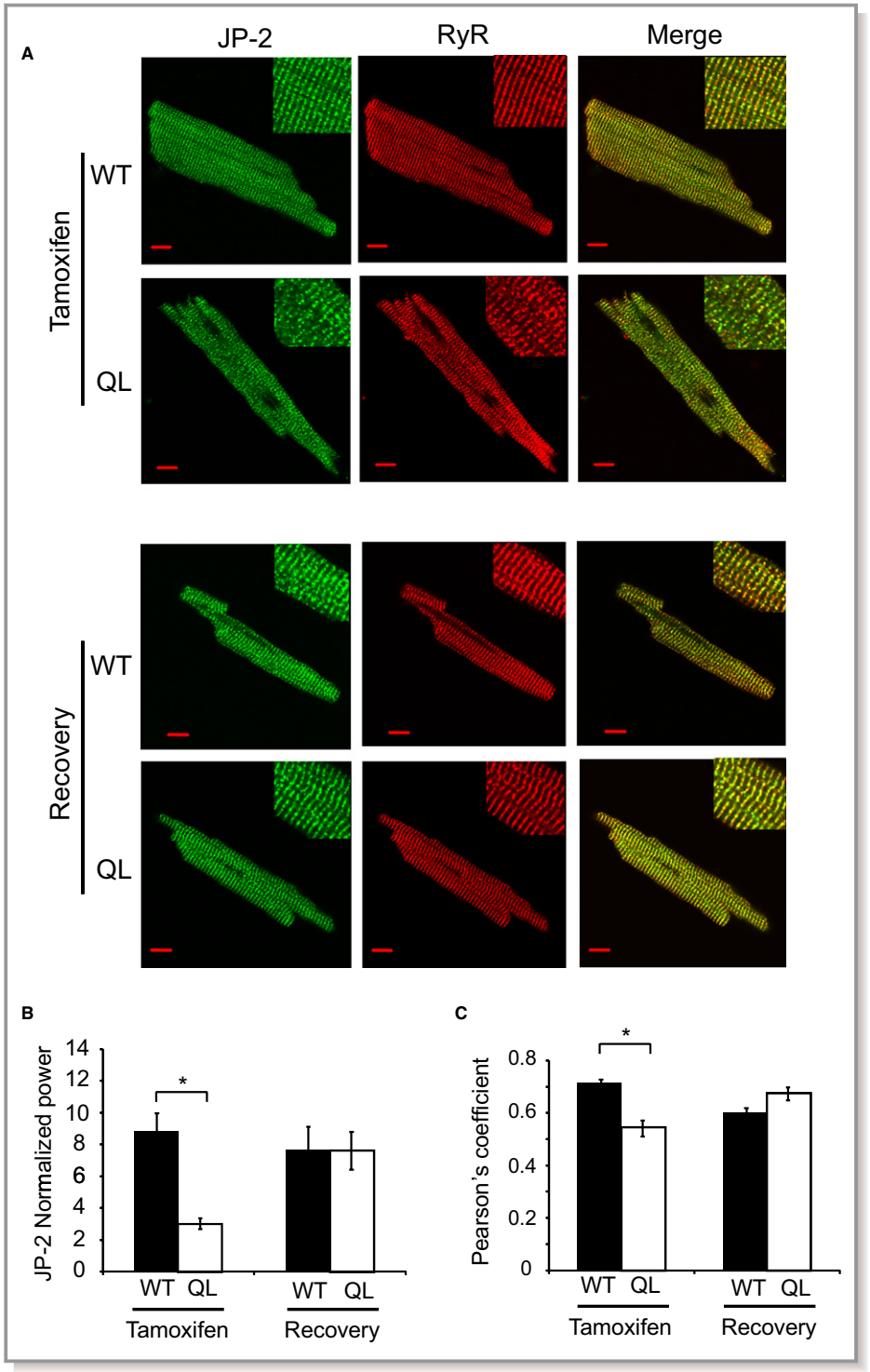

Figure 6. Mislocalization of JP-2 in QL myocytes. A, Representative immunofluorescence confocal microscopy images of myocytes prepared from WT and QL mice after 2 weeks of tamoxifen treatment (Tamoxifen) or 3 weeks after the last tamoxifen injection (Recovery). Cells were colabeled with antibodies against JP-2 (green) and RyR (red). Scale bars are 10 μm. B, Normalized power spectra calculated from one-dimensional Fourier transform of the JP-2 signal to analyze its spatial organization. Data are mean±SEM (*P<0.01, Student's t test; n=19 WT-tamoxifen cells; n=32 QL-tamoxifen cells; n=14 WT-recovery cells; n=18 QL-recovery cells; ≥3 hearts per group). C, Pearson's coefficient for colocalization of JP-2 and RyR. Data are mean±SEM (*P<0.01, Student's t test; n=19 WT-tamoxifen cells; n=29 QL-tamoxifen cells; n=13 WT-recovery cells; n=14 QL-recovery cells; ≥3 hearts per group). JP-2 indicates junctophilin-2; WT, wild-type.

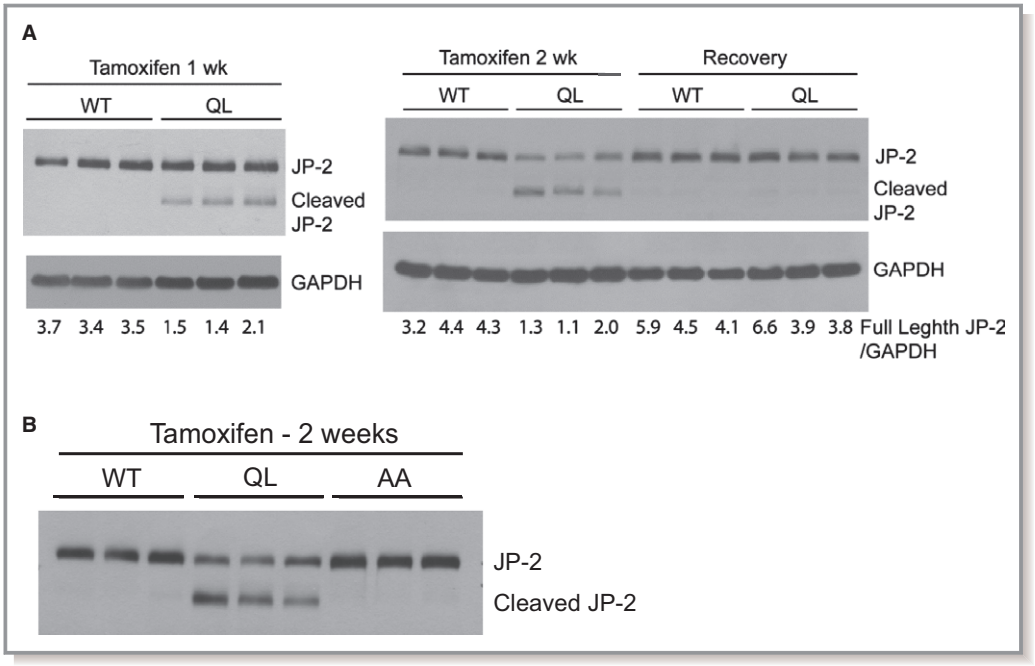

Figure 7. JP-2 cleavage in QL but not AA hearts. A, Heart lysates prepared from WT and QL mice after 1 or 2 weeks of tamoxifen injections (Tamoxifen) or 3 weeks after the last tamoxifen injection (Recovery) were analyzed by Western blotting for JP-2. GAPDH served as a loading control. Number below the blots are values obtained from quantification of full-length JP-2 bands normalized to GAPDH. QL is statistically different from WT after 1 or 2 weeks of tamoxifen injection ($P<0.05$), whereas QL-recovery is not statistically different from WT-recovery by Mann–Whitney *U*-test. B, Cleavage of JP-2 in QL but not AA hearts. Heart lysates prepared from WT, QL, and AA mice treated with tamoxifen for 2 weeks were analyzed by Western blotting for JP-2. GAPDH indicates glyceraldehyde 3-phosphate dehydrogenase; JP-2, junctophilin-2; WT, wild-type.

Activation of Calpain and Cleavage of JP-2

To further investigate the mechanism by which $G\alpha_q$ induces JP-2 cleavage, we used proteomics to analyze the JP-2 protein in the QL heart after 2 weeks of tamoxifen injections. JP-2 proteins were immunoprecipitated from heart lysates and then resolved by SDS-PAGE. Full-length and cleaved forms of JP-2 were cut out of the gel and digested with trypsin. Analysis of the tryptic peptides by mass spectroscopy revealed a unique polypeptide in the sample of cleaved JP-2 whose amino-terminal leucine is not adjacent to a trypsin cleavage site (Figure 8A and 8B, sequence in red). The cleavage site at the amino terminus of this peptide is a potential calpain recognition site. No JP-2 peptides amino-terminal to this site were identified in the sample of cleaved JP-2, whereas such peptides were readily detected in the sample of full-length JP-2 (Figure 8B).

To further investigate the role of calpain in JP-2 cleavage, we measured calpain activity in heart lysates prepared from mice injected with tamoxifen. We found that the average calpain activity was 2-fold higher in QL hearts than in WT hearts after 1 week of injections and, after 2 weeks of treatment calpain activity in QL hearts, was >2-fold higher than in the corresponding WT group (Figure 9A). Consistent with the increase in calpain activity, we detected a significant increase in the cleaved form of α-fodrin, a previously known calpain cleavage substrate,[41–43] in QL hearts (Figure 9B). In contrast, AA hearts, did not have higher calpain activity than WT hearts (Figure 9A). Western blots of heart lysates showed that the amount of calpain 1 protein in QL-tamoxifen samples was lower than in WT-tamoxifen or AA-tamoxifen samples, indicating that the increase in activity must be due to QL-dependent activation of the enzyme (Figure 10A). We also analyzed the heart samples by western blotting for calpastatin and did not detect a significant change in levels upon activation of $G\alpha_q$ (Figure 10B). Next, we injected QL mice for 2 weeks with calpain inhibitor III (reported to be selective for calpains I and II[31]) together with tamoxifen and found that cleavage of JP-2 was almost completely blocked in the calpain inhibitor-treated mice (Figure 11A). The inhibitor also protected myocytes from the deleterious effects of $G\alpha_q$ activation on T-tubule organization and JP-2 and RyR colocalization (Figure 11B and 11C). Importantly, cardiac contractile function was also protected in QL mice treated with tamoxifen plus the calpain inhibitor (Table 1). Taken together, these results strongly suggest that activation of calpain by $G\alpha_q$ leads to cleavage of JP-2 in cardiac myocytes, resulting in T-tubule disruption, Ca^{2+} handling dysfunction, and then heart failure.

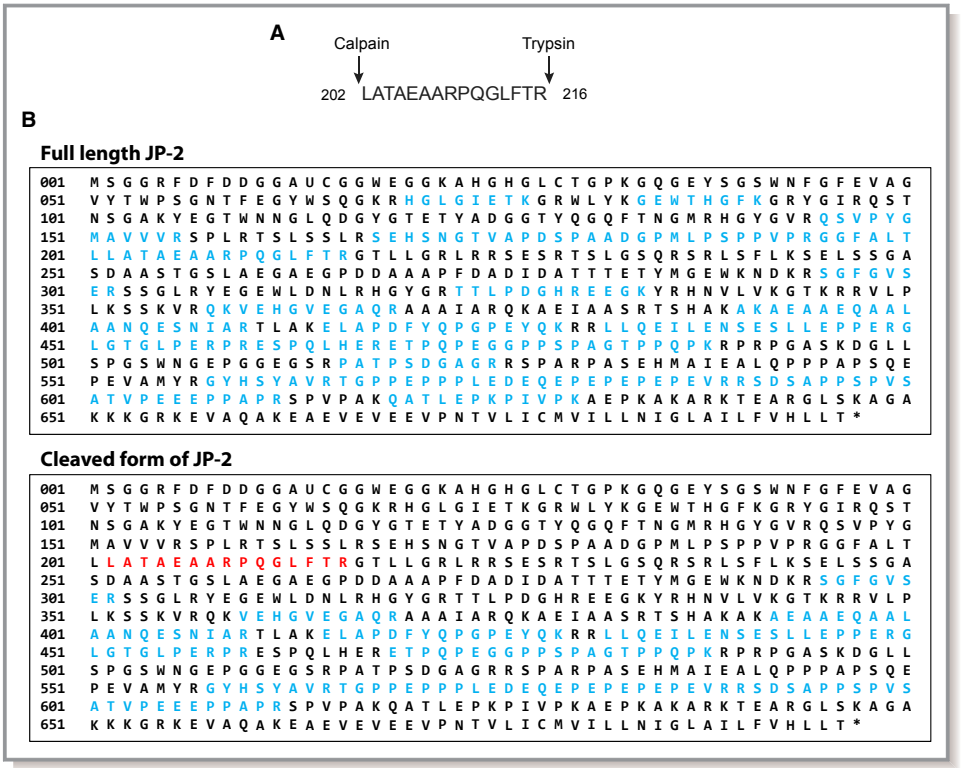

Figure 8. Proteomics analysis to determine the cleavage site in JP-2 from QL hearts. A, Proteomics analysis identified a unique tryptic peptide in the sample of cleaved JP-2 from QL-tamoxifen 2-week hearts. The amino terminus was potentially generated by cleavage by the calcium-dependent protease calpain. B, Full-length and cleaved forms of JP-2 were immunoprecipitated from QL-tamoxifen hearts, purified by SDS-PAGE, and digested with trypsin. Peptides in both samples were identified by mass spectroscopy. In blue are peptides identified in each preparation. In red is the peptide identified in the cleaved JP-2 sample that does not have a trypsin cleavage site next to the amino terminal leucine. JP-2 indicates junctophilin-2.

Discussion

Studies from many groups have provided compelling evidence that T-tubule remodeling is a common pathological alteration in failing myocytes of almost all origins, including different animal heart failure models of different species and etiologies and human heart failure patients with different cardiac etiologies (see Table 1 of ref. [40]). It is now also clear that T-tubule remodeling is not a secondary modification after heart failure but rather an important early ultrastructural alteration that contributes to the development of heart failure.[15] Disruption of this myocyte ultrastructure causes abnormalities of Ca^{2+} handling such as dyssynchrony and reduction of SR Ca^{2+} release, leading to myocyte contractile dysfunction and development of heart failure in various heart diseases.[5,8,10,11,15,16,44–46] More recent studies suggested that JP-2 downregulation is a key mechanism underlying T-tubule alterations in heart failure.[15,17] JP-2 expression levels are reduced in failing hearts,[15,16,19–22] and acute genetic knockdown of JP-2 by approximately 50% to 60% in cardiomyocytes in adult mice leads to T-tubule disorganization[15,17] and the development of acute heart failure.[17] In particular, this phenotype was observed despite suboptimal JP2 silencing in adult hearts, which was rescued by cardiac specific overexpression of JP2.[17] Although there are other mechanisms that contribute to the heart failure phenotype (as discussed next), these previous reports support the notion that the signaling cascade of JP-2 downregulation → T-tubule remodeling → Ca^{2+} handling dysfunction constitutes an important mechanism responsible for cardiac contractile failure in heart disease. Until now, the mechanisms underlying JP-2 dysregulation in heart failure remained incompletely understood.

In this study, using a mouse model of $G\alpha_q$-dependent reversible heart failure, we provide compelling evidence that turning on $G\alpha_q$ induces calpain activation, JP-2 cleavage (at the site of L201-L202), T-tubule disruption, Ca^{2+} transient defects, and heart failure. On the contrary, turning off $G\alpha_q$ reverses all of these events. Moreover, treatment of mice with a calpain inhibitor prevents $G\alpha_q$-dependent JP-2 cleavage, T-tubule disruption, and the development of heart failure. Thus, our data establish that $G\alpha_q$-dependent activation of calpain and subsequent calpain-dependent proteolysis of JP-2

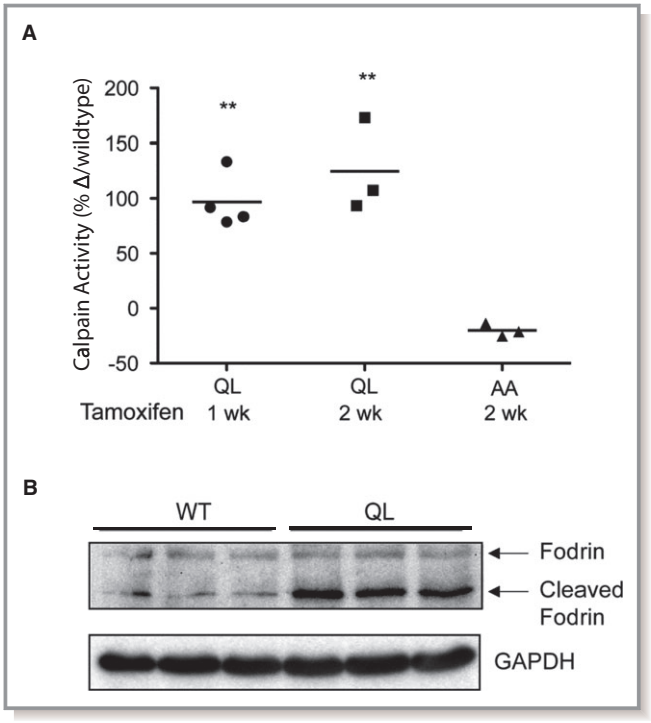

Figure 9. Increased calpain activity in QL hearts. A, Calpain activity was measured with heart lysates. Data shown are values for individual experiments, and the bar shown is the mean change of each group compared with WT group for each condition. $^{**}P<0.05$ by Mann–Whitney *U*-test for the differences between WT and QL paired group injected with tamoxifen for 1 or 2 weeks. Another paired group of WT and QL-AA mice were injected with tamoxifen for 2 weeks and the difference is not statistically significant (Mann–Whitney *U*-test). B, WT and QL mice were injected with tamoxifen for 2 weeks and the heart lysates analyzed for cleavage of fodrin by Western blotting. WT indicates wild-type.

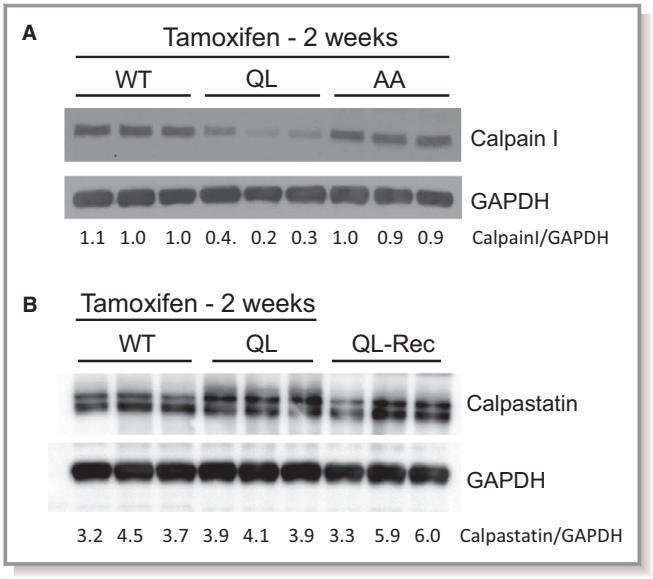

Figure 10. Calpain and calpastatin expression levels in the QL hearts. Heart lysates prepared from WT and QL mice treated with tamoxifen for 2 weeks were analyzed by Western blotting for calpain I (A) or calpastatin (B). GAPDH was used as loading control. Number below the blots are values obtained from quantification of bands normalized to GAPDH. A, QL is statistically different from WT ($P<0.05$) by Mann–Whitney *U*-test. B, The 3 groups are not statistically different by Kruskal–Wallis test. GAPDH indicates glyceraldehyde 3-phosphate dehydrogenase; WT, wild-type.

are important molecular mechanisms that contribute to T-tubule remodeling, Ca^{2+} handling dysfunction, and progression to heart failure in this mouse model. Our data revealed a post-translational mechanism—that is, calpain-mediated JP-2 proteolysis—involved in JP-2 dysregulation in heart failure. This finding is complementary to miR-24–mediated post-transcriptional regulation of JP-2 expression, as recently discovered by Wang and his colleagues,[23–25] and microtubule-mediated defects in JP-2 trafficking that also contribute to T-tubule remodeling and the development of heart failure.[47]

Many studies have implicated β-adrenergic and angiotensin II G protein–coupled receptor signaling in Ca^{2+}-mediated calpain activation in failing hearts.[48,49] Because we use a model of constitutive $G\alpha_q$ signaling, we speculate that the mechanism of calpain activation is similar to that reported in previous studies (ie, through a common mechanism of Ca^{2+} elevation). Active $G\alpha_q$ binds and stimulates PLCβ to produce diacylglycerol and IP_3 from phosphatidylinositol-4,5-bisphosphate.[39] IP_3 binds to IP_3 receptors (IP_3Rs) to stimulate the release of Ca^{2+} from the endoplasmic reticulum or the nuclear envelope.[50] Our results using the AA mouse strain indicate activation of PLCβ is required to activate calpain to cleave JP-2. Multiple pieces of evidence indicate that enhancement of IP_3–IP_3R signaling alters cardiac excitation-contraction coupling; that is, it increases the systolic global Ca^{2+} transient and elevates the diastolic Ca^{2+} level.[51–53] Based on the results from our study, one may surmise that $G\alpha_q$-induced IP_3 mediated Ca^{2+} release that could lead to activation of calpain, which then cleaves JP-2 to cause the observed phenotype. However, our results do not rule out the possibility that PLCβ could be regulating calpain through a protein kinase C pathway. Future studies that determine the downstream signaling events after PLCβ activation will provide new mechanistic information to fill this gap in knowledge. In addition, studies are needed to characterize the intracellular location(s) where JP-2 is cleaved by activated calpain.

It is also unclear why calpain activity is increased despite a decrease in expression of calpain I. Regulation of calpain activity is complex and not completely understood. We speculate that the decrease in calpain I expression is a compensatory response by the myocytes to turn off the deleterious effects of calpain activation. Downexpression of calpastatin, the endogenous calpain inhibitor, is also not responsible for the increased calpain activity. We postulate that changes in calpain localization, which have been

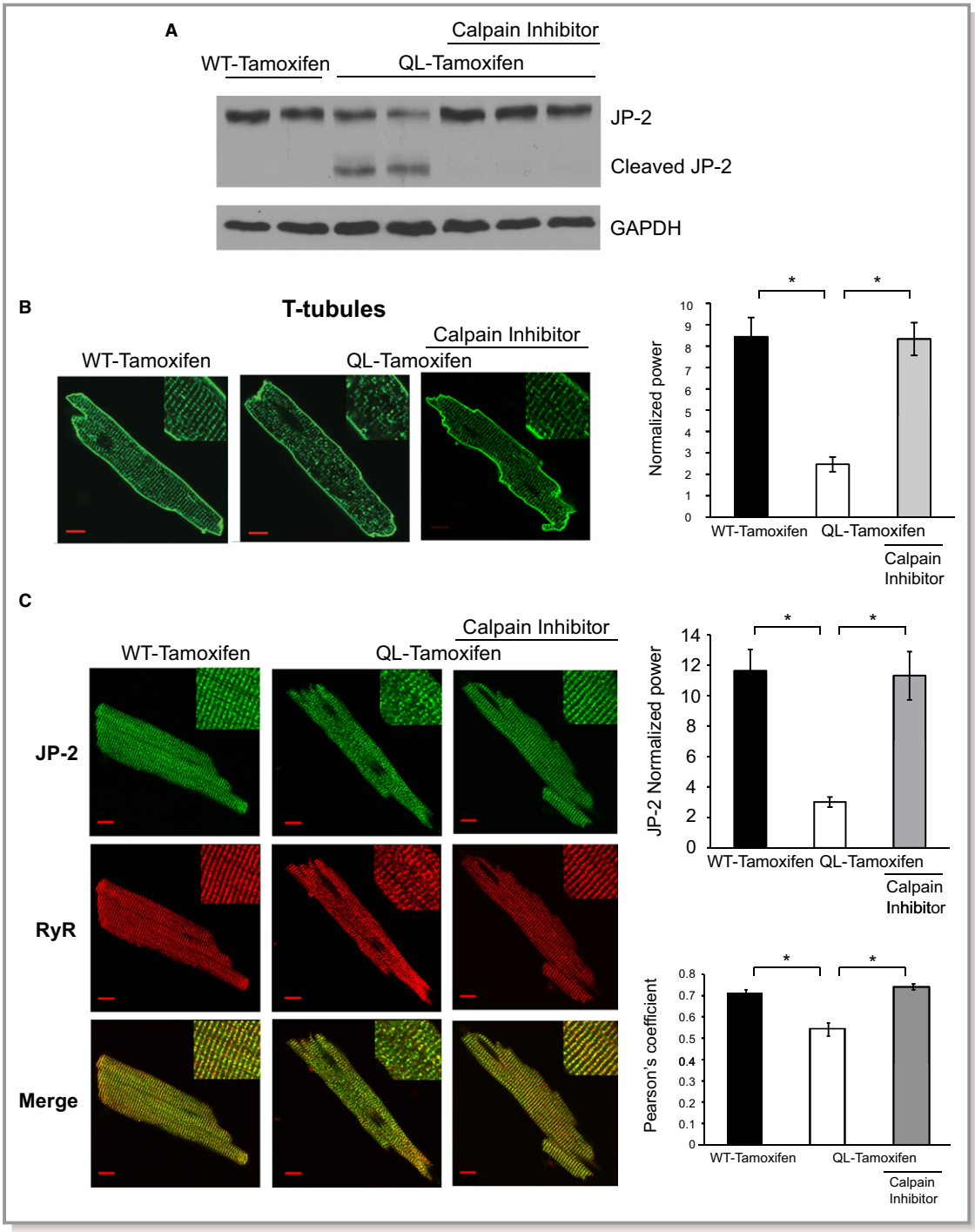

Figure 11. Inhibition of JP-2 cleavage in QL hearts by a calpain inhibitor. WT and QL mice were injected daily with tamoxifen (1 mg) plus or minus calpain inhibitor III (500 μg) for 2 weeks. A, Heart lysates were analyzed by western blotting for JP-2. The blot was reprobed for GAPDH as a loading control. B, Ventricular myocytes were isolated and stained with di-8-ANEPPS for the T-tubule structure. Representative confocal microscopy images are shown. Scale bars are 10 μm. The bar graph shows normalized peak power (at the dominant frequency) computed from one-dimensional Fourier analysis of the di-8-ANEPPS signal as a measure of T-tubule spatial organization. Data are mean±SEM (*P<0.01, one-way ANOVA with Bonferroni post test; n=22 to 27 cells from ≥3 hearts per group). C, Ventricular myocytes were isolated and stained with antibody against JP-2 and RyR. Representative immunofluorescence confocal microscopy images are shown. Scale bars are 10 μm. The bar graph shows normalized peak power of the JP-2 signal to analyze its spatial organization. The bottom bar graph shows the Pearson's coefficient of JP-2/RyR colocalization. Data are mean±SEM (*P<0.01, one-way ANOVA with Bonferroni post-test; n=16 to 29 cells from ≥3 hearts per group). GAPDH indicates glyceraldehyde 3-phosphate dehydrogenase; JP-2, junctophilin-2; WT, wild-type.

associated with differential calpain activity,[44,45] may be responsible for the increase in calpain activity. Imaging studies that examine the cellular location of calpain isoforms in isolated myocytes following acute activation of Gαq could be informative.

The mechanisms by which withdrawal of tamoxifen restores cardiac function remain incompletely elucidated. We have previously reported that withdrawal of tamoxifen in QL mice normalizes L-type Ca^{2+} channel activity,[29] which, taken with the present study, is likely through restoration of T-tubule architecture. Based on the mechanism we uncovered for T-tubule remodeling in QL hearts, we would presume that, with tamoxifen withdrawal and normalization of Gαq signaling, a decrease in calpain activity precedes restoration of JP2 expression, T-tubule ultrastructure and synchronous SR Ca^{2+} release.

A number of studies have now shown that the disrupted T-tubule structure can be restored by increasing the expression of SERCA2, exercise, cardiac resynchronization therapy or mechanical unloading,[5,21,54–56] suggesting that the T-tubule network is a dynamic, regulated structure. In the present study, we conclusively demonstrate that the restoration of T-tubule ultrastructure is possible once the insulting stimulus causing the disruption is terminated. Our results suggest that the molecular mechanism responsible for this remodeling cycle is the onset and termination of JP-2 proteolysis.

Heart failure is a complex multifaceted syndrome as heart disease of different etiologies approaches end stage. In addition to T-tubule (ultra)structural remodeling, many other mechanisms, including β-adrenergic receptor unresponsiveness, oxidative stress, protein kinase C activation, SR calcium handling abnormalities, metabolic inhibition, mitochondria dysfunction, and so on, are also critically involved in the pathogenesis of heart failure. It is possible that constitutive activation of $G\alpha_q$ also contributes to some or all of these pathogenic pathways. For example, constitutive $G\alpha_q$ activation may also alter RyR2 organization, although, as far as we know, there is no evidence in the literature that $G\alpha_q$ signaling regulates RyR2 organization. T-tubule remodeling may cause redistribution and loss of β-adrenergic receptors in the T-tubules in failing cardiomyocytes.[54,57] Thus, our findings complement previous findings and provide new insights into the mechanistic role of myocyte ultrastructural alterations in heart failure development and progression.

Each of the key steps of the signaling cascade "Gαq activation → elevation of calpain activity → JP-2 dysregulation → T-tubule remodeling → heart failure" is known to be a common alteration existing in many forms of heart disease. For example, many studies have established that $G\alpha_q$ signaling plays a critical role in the development of cardiac hypertrophy and heart failure.[26,27] Calpain activity has also been found to be increased in a variety of pathological conditions.[58–63] Our study provides evidence of a sequential mechanistic linkage among these events and therefore provides new insights into our understanding of heart failure pathogenesis in general heart disease. The fact that disrupted T-tubule networks can undergo repair, plus the ability of the calpain inhibitor to block T-tubule disruption, holds promise for the development of interventions to modulate JP-2 levels as a treatment for heart failure. Drugs and nonpharmacological approaches designed to block the degradation or enhance the level of JP-2 may improve the contractile dysfunction in heart failure.

In summary, our data reveal that T-tubule structural remodeling is a reversible process that mirrors the status of cardiac function. Calpain-mediated JP-2 proteolysis represents the molecular mechanism by which JP-2 is degraded, leading to T-tubule disruption, Ca^{2+} handling dysfunction, and progression of heart failure.

Acknowledgments

We thank Lisa Ballou for her helpful discussion and editing of the manuscript. We also thank Sergey Doronin for his assistance with the calpain activity assay, and Kay Chen for her assistant with the data analysis of JP-2 and RyR colocalization.

Sources of Funding

This study was funded in part by grants from the Department of Veterans Affairs Merit Review Program (to Dr Lin), the American Heart Association (0635056N to Dr Song), and the National Institutes of Health (DK62722 and CA136754 to Dr Lin; HL090905 to Dr Song).

Disclosures

None.

References

1. Roger VL, Go AS, Lloyd-Jones DM, Benjamin EJ, Berry JD, Borden WB, Bravata DM, Dai S, Ford ES, Fox CS, Fullerton HJ, Gillespie C, Hailpern SM, Heit JA, Howard VJ, Kissela BM, Kittner SJ, Lackland DT, Lichtman JH, Lisabeth LD, Makuc DM, Marcus GM, Marelli A, Matchar DB, Moy CS, Mozaffarian D, Mussolino ME, Nichol G, Paynter NP, Soliman EZ, Sorlie PD, Sotoodehnia N, Turan TN, Virani SS, Wong ND, Woo D, Turner MB. Heart disease and stroke statistics–2012 update: a report from the American Heart Association. *Circulation*. 2012;125:e2–e220.
2. Woodcock EA, Grubb DR, Iliades P. Potential treatment of cardiac hypertrophy and heart failure by inhibiting the sarcolemmal binding of phospholipase Cbeta1b. *Curr Drug Targets*. 2010;11:1032–1040.
3. Soeller C, Cannell MB. Examination of the transverse tubular system in living cardiac rat myocytes by 2-photon microscopy and digital image-processing techniques. *Circ Res*. 1999;84:266–275.
4. Brette F, Orchard C. T-tubule function in mammalian cardiac myocytes. *Circ Res*. 2003;92:1182–1192.
5. Sachse FB, Torres NS, Savio-Galimberti E, Aiba T, Kass DA, Tomaselli GF, Bridge JH. Subcellular structures and function of myocytes impaired during heart failure are restored by cardiac resynchronization therapy. *Circ Res*. 2012;110:588–597.

6. Lyon AR, MacLeod KT, Zhang Y, Garcia E, Kanda GK, Lab MJ, Korchev YE, Harding SE, Gorelik J. Loss of T-tubules and other changes to surface topography in ventricular myocytes from failing human and rat heart. *Proc Natl Acad Sci USA*. 2009;106:6854–6859.
7. He J, Conklin MW, Foell JD, Wolff MR, Haworth RA, Coronado R, Kamp TJ. Reduction in density of transverse tubules and L-type Ca(2+) channels in canine tachycardia-induced heart failure. *Cardiovasc Res*. 2001;49:298–307.
8. Balijepalli RC, Kamp TJ. Cardiomyocyte transverse tubule loss leads the way to heart failure. *Future Cardiol*. 2011;7:39–42.
9. Crossman DJ, Ruygrok PN, Soeller C, Cannell MB. Changes in the organization of excitation-contraction coupling structures in failing human heart. *PLoS ONE*. 2011;6:e17901.
10. Heinzel FR, Bito V, Biesmans L, Wu M, Detre E, von Wegner F, Claus P, Dymarkowski S, Maes F, Bogaert J, Rademakers F, D'Hooge J, Sipido K. Remodeling of T-tubules and reduced synchrony of Ca2+ release in myocytes from chronically ischemic myocardium. *Circ Res*. 2008;102:338–346.
11. Louch WE, Mork HK, Sexton J, Stromme TA, Laake P, Sjaastad I, Sejersted OM. T-tubule disorganization and reduced synchrony of Ca2+ release in murine cardiomyocytes following myocardial infarction. *J Physiol*. 2006; 574:519–533.
12. Balijepalli RC, Lokuta AJ, Maertz NA, Buck JM, Haworth RA, Valdivia HH, Kamp TJ. Depletion of T-tubules and specific subcellular changes in sarcolemmal proteins in tachycardia-induced heart failure. *Cardiovasc Res*. 2003;59:67–77.
13. Brette F, Despa S, Bers DM, Orchard CH. Spatiotemporal characteristics of SR Ca(2+) uptake and release in detubulated rat ventricular myocytes. *J Mol Cell Cardiol*. 2005;39:804–812.
14. Yang Z, Pascarel C, Steele DS, Komukai K, Brette F, Orchard CH. Na+-Ca2+ exchange activity is localized in the T-tubules of rat ventricular myocytes. *Circ Res*. 2002;91:315–322.
15. Wei S, Guo A, Chen B, Kutschke W, Xie YP, Zimmerman K, Weiss RM, Anderson ME, Cheng H, Song LS. T-tubule remodeling during transition from hypertrophy to heart failure. *Circ Res*. 2010;107:520–531.
16. Wu CY, Jia Z, Wang W, Ballou LM, Jiang YP, Chen B, Mathias RT, Cohen IS, Song LS, Entcheva E, Lin RZ. PI3Ks maintain the structural integrity of T-tubules in cardiac myocytes. *PLoS ONE*. 2011;6:e24404.
17. van Oort RJ, Garbino A, Wang W, Dixit SS, Landstrom AP, Gaur N, De Almeida AC, Skapura DG, Rudy Y, Burns AR, Ackerman MJ, Wehrens XH. Disrupted junctional membrane complexes and hyperactive ryanodine receptors after acute junctophilin knockdown in mice. *Circulation*. 2011;123:979–988.
18. Takeshima H, Komazaki S, Nishi M, Iino M, Kangawa K. Junctophilins: a novel family of junctional membrane complex proteins. *Mol Cell*. 2000;6:11–22.
19. Minamisawa S, Oshikawa J, Takeshima H, Hoshijima M, Wang Y, Chien KR, Ishikawa Y, Matsuoka R. Junctophilin type 2 is associated with caveolin-3 and is down-regulated in the hypertrophic and dilated cardiomyopathies. *Biochem Biophys Res Commun*. 2004;325:852–856.
20. Xu M, Zhou P, Xu SM, Liu Y, Feng X, Bai SH, Bai Y, Hao XM, Han Q, Zhang Y, Wang SQ. Intermolecular failure of L-type Ca2+ channel and ryanodine receptor signaling in hypertrophy. *PLoS Biol*. 2007;5:e21.
21. Xie YP, Chen B, Sanders P, Guo A, Li Y, Zimmerman K, Wang LC, Weiss RM, Grumbach IM, Anderson ME, Song LS. Sildenafil prevents and reverses transverse-tubule remodeling and Ca(2+) handling dysfunction in right ventricle failure induced by pulmonary artery hypertension. *Hypertension*. 2012;59:355–362.
22. Chen B, Li Y, Jiang S, Xie YP, Guo A, Kutschke W, Zimmerman K, Weiss RM, Miller FJ, Anderson ME, Song LS. beta-Adrenergic receptor antagonists ameliorate myocyte T-tubule remodeling following myocardial infarction. *FASEB J*. 2012;26:2531–2537.
23. Xu M, Wu HD, Li RC, Zhang HB, Wang M, Tao J, Feng XH, Guo YB, Li SF, Lai ST, Zhou P, Li LL, Yang HQ, Luo GZ, Bai Y, Xi JJ, Gao W, Han QD, Zhang YY, Wang XJ, Meng X, Wang SQ. Mir-24 regulates junctophilin-2 expression in cardiomyocytes. *Circ Res*. 2012;111:837–841.
24. Li RC, Tao J, Guo YB, Wu HD, Liu RF, Bai Y, Lv ZZ, Luo GZ, Li LL, Wang M, Yang HQ, Gao W, Han QD, Zhang YY, Wang XJ, Xu M, Wang SQ. In vivo suppression of microRNA-24 prevents the transition toward decompensated hypertrophy in aortic-constricted mice. *Circ Res*. 2013;112:601–605.
25. Song LS, Guo A, Lin RZ. MicroRNA: a toolkit fine-tuning the dyadic "fuzzy space"? *Circ Res*. 2012;111:816–818.
26. Dorn GW 2nd, Brown JH. Gq signaling in cardiac adaptation and maladaptation. *Trends Cardiovasc Med*. 1999;9:26–34.
27. Akhter SA, Luttrell LM, Rockman HA, Iaccarino G, Lefkowitz RJ, Koch WJ. Targeting the receptor-Gq interface to inhibit in vivo pressure overload myocardial hypertrophy. *Science*. 1998;280:574–577.
28. D'Angelo DD, Sakata Y, Lorenz JN, Boivin GP, Walsh RA, Liggett SB, Dorn GW 2nd. Transgenic Galphaq overexpression induces cardiac contractile failure in mice. *Proc Natl Acad Sci USA*. 1997;94:8121–8126.
29. Jiang YP, Ballou LM, Lu Z, Li W, Kelly DJ, Cohen IS, Lin RZ. Reversible heart failure in G alpha(q) transgenic mice. *J Biol Chem*. 2006;281:29988–29992.
30. Fan G, Jiang YP, Lu Z, Martin DW, Kelly DJ, Zuckerman JM, Ballou LM, Cohen IS, Lin RZ. A transgenic mouse model of heart failure using inducible Galpha q. *J Biol Chem*. 2005;280:40337–40346.
31. Mehdi S. Cell-penetrating inhibitors of calpain. *Trends Biochem Sci*. 1991;16:150–153.
32. Lu Z, Jiang YP, Xu XH, Ballou LM, Cohen IS, Lin RZ. Decreased L-type Ca2+ current in cardiac myocytes of type 1 diabetic Akita mice due to reduced phosphatidylinositol 3-kinase signaling. *Diabetes*. 2007;56:2780–2789.
33. Lu Z, Jiang YP, Wang W, Xu XH, Mathias RT, Entcheva E, Ballou LM, Cohen IS, Lin RZ. Loss of cardiac phosphoinositide 3-kinase p110 alpha results in contractile dysfunction. *Circulation*. 2009;120:318–325.
34. Aistrup GL, Kelly JE, Kapur S, Kowalczyk M, Sysman-Wolpin I, Kadish AH, Wasserstrom JA. Pacing-induced heterogeneities in intracellular Ca2+ signaling, cardiac alternans, and ventricular arrhythmias in intact rat heart. *Circ Res*. 2006;99:e65–e73.
35. Rubart M, Wang E, Dunn KW, Field LJ. Two-photon molecular excitation imaging of Ca2+ transients in Langendorff-perfused mouse hearts. *Am J Physiol Cell Physiol*. 2003;284:C1654–C1668.
36. Song LS, Guia A, Muth JN, Rubio M, Wang SQ, Xiao RP, Josephson IR, Lakatta EG, Schwartz A, Cheng H. Ca(2+) signaling in cardiac myocytes overexpressing the alpha(1) subunit of L-type Ca(2+) channel. *Circ Res*. 2002;90:174–181.
37. Tanner S, Shu H, Frank A, Wang LC, Zandi E, Mumby M, Pevzner PA, Bafna V. InsPecT: identification of posttranslationally modified peptides from tandem mass spectra. *Anal Chem*. 2005;77:4626–4639.
38. Yano M, Ikeda Y, Matsuzaki M. Altered intracellular Ca2+ handling in heart failure. *J Clin Investig*. 2005;115:556–564.
39. Mizuno N, Itoh H. Functions and regulatory mechanisms of Gq-signaling pathways. *Neurosignals*. 2009;17:42–54.
40. Guo A, Zhang C, Wei S, Chen B, Song LS. Emerging mechanisms of T-tubule remodelling in heart failure. *Cardiovasc Res*. 2013;98:204–215.
41. Barta J, Toth A, Edes I, Vaszily M, Papp JG, Varro A, Papp Z. Calpain-1-sensitive myofibrillar proteins of the human myocardium. *Mol Cell Biochem*. 2005;278:1–8.
42. Goncalves I, Nitulescu M, Saido TC, Dias N, Pedro LM, E Fernandes JF, Ares MP, Porn-Ares I. Activation of calpain-1 in human carotid artery atherosclerotic lesions. *BMC Cardiovasc Disord*. 2009;9:26.
43. Scheubel RJ, Bartling B, Simm A, Silber RE, Drogaris K, Darmer D, Holtz J. Apoptotic pathway activation from mitochondria and death receptors without caspase-3 cleavage in failing human myocardium: fragile balance of myocyte survival? *J Am Coll Cardiol*. 2002;39:481–488.
44. Ibrahim M, Gorelik J, Yacoub MH, Terracciano CM. The structure and function of cardiac t-tubules in health and disease. *Proc Biol Sci*. 2011;278:2714–2723.
45. Song LS, Sobie EA, McCulle S, Lederer WJ, Balke CW, Cheng H. Orphaned ryanodine receptors in the failing heart. *Proc Natl Acad Sci USA*. 2006; 103:4305–4310.
46. Lenaerts I, Bito V, Heinzel FR, Driesen RB, Holemans P, D'Hooge J, Heidbuchel H, Sipido KR, Willems R. Ultrastructural and functional remodeling of the coupling between Ca2+ influx and sarcoplasmic reticulum Ca2+ release in right atrial myocytes from experimental persistent atrial fibrillation. *Circ Res*. 2009;105:876–885.
47. Zhang C, Chen B, Guo A, Zhu Y, Miller JD, Gao S, Yuan C, Kutschke W, Zimmerman K, Weiss RM, Wehrens XH, Hong J, Johnson FL, Santana LF, Anderson ME, Song LS. Microtubule-mediated defects in junctophilin-2 trafficking contribute to myocyte T-tubule remodeling and Ca2+ handling dysfunction in heart failure. *Circulation*. 2014;129:1742–1750.
48. Zatz M, Starling A. Calpains and disease. *N Engl J Med*. 2005;352:2413–2423.
49. Goll DE, Thompson VF, Li H, Wei W, Cong J. The calpain system. *Physiol Rev*. 2003;83:731–801.
50. Wu X, Zhang T, Bossuyt J, Li X, McKinsey TA, Dedman JR, Olson EN, Chen J, Brown JH, Bers DM. Local InsP3-dependent perinuclear Ca2+ signaling in cardiac myocyte excitation-transcription coupling. *J Clin Investig*. 2006; 116:675–682.
51. Harzheim D, Movassagh M, Foo RS, Ritter O, Tashfeen A, Conway SJ, Bootman MD, Roderick HL. Increased InsP3Rs in the junctional sarcoplasmic reticulum augment Ca2+ transients and arrhythmias associated with cardiac hypertrophy. *Proc Natl Acad Sci USA*. 2009;106:11406–11411.

52. Li X, Zima AV, Sheikh F, Blatter LA, Chen J. Endothelin-1-induced arrhythmogenic Ca2+ signaling is abolished in atrial myocytes of inositol-1,4,5-trisphosphate(IP3)-receptor type 2-deficient mice. *Circ Res*. 2005;96:1274–1281.

53. Zima AV, Blatter LA. Inositol-1,4,5-trisphosphate-dependent Ca(2+) signalling in cat atrial excitation-contraction coupling and arrhythmias. *J Physiol*. 2004;555:607–615.

54. Lyon AR, Nikolaev VO, Miragoli M, Sikkel MB, Paur H, Benard L, Hulot JS, Kohlbrenner E, Hajjar RJ, Peters NS, Korchev YE, Macleod KT, Harding SE, Gorelik J. Plasticity of surface structures and beta(2)-adrenergic receptor localization in failing ventricular cardiomyocytes during recovery from heart failure. *Circ Heart Fail*. 2012;5:357–365.

55. Kemi OJ, Hoydal MA, Macquaide N, Haram PM, Koch LG, Britton SL, Ellingsen O, Smith GL, Wisloff U. The effect of exercise training on transverse tubules in normal, remodeled, and reverse remodeled hearts. *J Cell Physiol*. 2011;226:2235–2243.

56. Ibrahim M, Terracciano CM. Reversibility of T-tubule remodelling in heart failure: mechanical load as a dynamic regulator of the T-tubules. *Cardiovasc Res*. 2013;98:225–232.

57. Nikolaev VO, Moshkov A, Lyon AR, Miragoli M, Novak P, Paur H, Lohse MJ, Korchev YE, Harding SE, Gorelik J. Beta2-adrenergic receptor redistribution in heart failure changes cAMP compartmentation. *Science*. 2010;327:1653–1657.

58. Greyson CR, Schwartz GG, Lu L, Ye S, Helmke S, Xu Y, Ahmad H. Calpain inhibition attenuates right ventricular contractile dysfunction after acute pressure overload. *J Mol Cell Cardiol*. 2008;44:59–68.

59. Sandmann S, Yu M, Unger T. Transcriptional and translational regulation of calpain in the rat heart after myocardial infarction–effects of AT(1) and AT(2) receptor antagonists and ACE inhibitor. *Br J Pharmacol*. 2001;132:767–777.

60. Arthur GD, Belcastro AN. A calcium stimulated cysteine protease involved in isoproterenol induced cardiac hypertrophy. *Mol Cell Biochem*. 1997;176:241–248.

61. Patterson C, Portbury AL, Schisler JC, Willis MS. Tear me down: role of calpain in the development of cardiac ventricular hypertrophy. *Circ Res*. 2011;109:453–462.

62. Li Y, Ma J, Zhu H, Singh M, Hill D, Greer PA, Arnold JM, Abel ED, Peng T. Targeted inhibition of calpain reduces myocardial hypertrophy and fibrosis in mouse models of type 1 diabetes. *Diabetes*. 2011;60:2985–2994.

63. Letavernier E, Perez J, Bellocq A, Mesnard L, de Castro Keller A, Haymann JP, Baud L. Targeting the calpain/calpastatin system as a new strategy to prevent cardiovascular remodeling in angiotensin II-induced hypertension. *Circ Res* 2008;102:720–728.